

# Continued slowing of the Ross Ice Shelf and thickening of West Antarctic ice streams

R. THOMAS,<sup>1</sup> B. SCHEUCHL,<sup>2</sup> E. FREDERICK,<sup>1</sup> R. HARPOLD,<sup>1</sup> C. MARTIN,<sup>1</sup>  
E. RIGNOT<sup>2,3</sup>

<sup>1</sup>*Sigma Space Inc., NASA Wallops Flight Center, Wallops Island, VA, USA*  
*E-mail: robert\_thomas@hotmail.com*

<sup>2</sup>*Department of Earth System Science, University of California–Irvine, Irvine, CA, USA*

<sup>3</sup>*Jet Propulsion Laboratory, California Institute of Technology, Pasadena, CA, USA*

**ABSTRACT.** As part of the Ross Ice Shelf Geophysical and Glaciological Survey (RIGGS), ice velocities were measured on the Ross Ice Shelf (RIS) during 1973–78. Comparisons of these with velocity estimates at the same locations derived from RADARSAT synthetic aperture radar (SAR) measurements in 1997 and 2009 show velocity reduction in the southeast quadrant of the ice shelf by almost  $200 \text{ m a}^{-1}$ , with deceleration rates increasing with time. Large areas of ice shelf in this region are lightly grounded, forming an ‘ice plain’ that increases local buttressing of the ice streams. ICESat measurements show this ice plain to be thickening. The observed decrease in ice-shelf velocities implies a total reduction in the mass of ice flowing into the RIS from the West Antarctic ice sheet (WAIS) by  $\sim 23 \text{ Gt a}^{-1}$ , shifting the mass balance of the WAIS drainage basin from strongly negative in the 1970s to strongly positive in 2009. The resulting decrease in ice advection should lead to ice-shelf thinning further seaward of the ice plain. This thinning would reduce the lateral drag and back-stress of the shelf ice, further contributing to thinning through an increase in spreading rate. ICESat measurements show recent thinning of most of the freely floating ice shelf.

## 1. INTRODUCTION

The Ross Ice Shelf (RIS) is fed by large glaciers and ice streams flowing from both East and West Antarctica, by snow falling on its surface and, to a lesser extent, by basal freezing. It loses ice by basal melting and the calving of icebergs from its seaward ice front. Between 1973 and 1978, as part of the Ross Ice Shelf Geophysical and Glaciological Survey (RIGGS), velocities and ice thicknesses were measured at 149 locations on the RIS, most of which formed a grid pattern (Bentley, 1984), with stations  $\sim 50 \text{ km}$  apart (Fig. 1). Soon afterwards, a long-term project was initiated to investigate the West Antarctic ice sheet (WAIS) ice streams, including measurements of velocities on both the ice streams and the ice shelf, and, in 1997 and 2009, velocities were also inferred from satellite synthetic aperture radar (SAR) measurements.

The WAIS discharges ice into the RIS along six large ice streams (Fig. 1). Shabtaie and Bentley (1987) used the RIGGS measurements to infer a negative mass balance of  $\sim 20 \text{ Gt a}^{-1}$  for the catchment regions of these ice streams. They also showed the inland ice to be more extensive than previously mapped, and that it includes a large, weakly grounded ‘ice plain’ in the southeast corner of the ice shelf that was thickening quite rapidly (Thomas, 1976). Later measurements showed slowing of the WAIS ice streams flowing into this region (e.g. Stephenson and Bindschadler, 1988; Joughin and others, 2002, 2005). Possible reasons include increased resistance to ice-stream flow by thickening regions of the ice plain (Thomas and others, 1988), and reduced basal lubrication on the ice streams (Hulbe and Fahnestock, 2004; Catania and others, 2006; Beem and others, 2010). Interpretations, primarily of remotely sensed data, reveal a longer history of major changes in the WAIS ice streams extending over the past 1000 years (e.g. Fahnestock and others, 2000; Catania and others, 2012), ranging from

complete shutdown to major accelerations. These changes altered the direction of ice flowing from the ice streams into the ice shelf, resulting in flowband orientations that differ from those consistent with present ice-stream behavior.

Here we compare the RIGGS measurements of RIS ice velocities with the SAR measurements in 1997 and 2009 to show continued velocity decrease in the southeast corner of the ice shelf, but little change near the calving ice front. This implies a decrease in ice drainage from the WAIS and in seaward advection of thicker ice from the southeast, and an increase in longitudinal stretching of much of the ice shelf, resulting in ice-shelf thinning. We also use the various measurements to infer a transition from strongly negative balance for the WAIS ice streams in the 1970s to substantial thickening by 2009. Between 2003 and 2009, NASA’s Ice, Cloud and land Elevation Satellite (ICESat) made accurate measurements of surface elevation over most of the Earth, including Antarctica, and we use these measurements to confirm recent thickening of the WAIS drainage basin, and slow thinning of much of the RIS.

## 2. OBSERVATIONS

RIGGS measurements included repeated position fixes at 64 stations, using satellite Doppler-tracking equipment (Geoceiver or JMR-1), from which ice-shelf velocities were inferred, with velocities interpolated to other stations using surface strain rates that were measured at all stations (Thomas and others, 1984). Estimated velocity errors ranged from a few  $\text{m a}^{-1}$  at the four base camps to  $30 \text{ m a}^{-1}$  for interpolated values. The RIGGS measurements were made over the 5 year period 1973–78, with a 1 year interval between Geoceiver and strain-rate measurements at most stations. Here we assign all these velocity estimates to 1975.

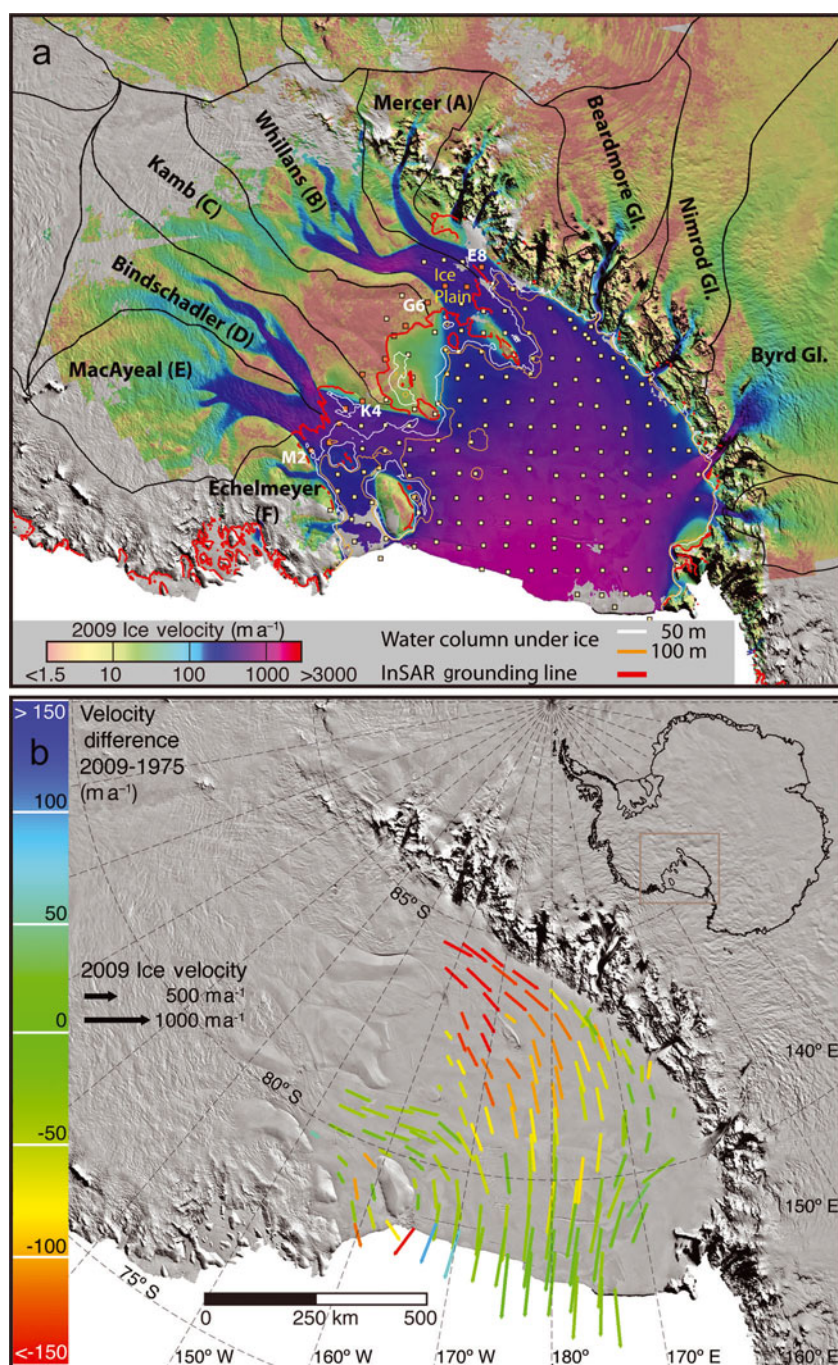


**Fig. 1.** (a) Locations of RIGGS stations, and ice streams flowing from the WAIS: Mercer, Whillans, Kamb, Bindschadler, MacAyeal and Echelmeyer ice streams. For convenience, we refer to these ice streams respectively as A–F (as in earlier published papers). We also include Beardmore, Nimrod and Byrd glaciers flowing from the East Antarctica ice sheet into the RIS. Red stations M2 to E8 show the transect across which velocities shown in Figure 2 were used to calculate total discharge from the WAIS into the RIS. The grounding line was inferred from InSAR data (Rignot and others, 2011). The white and orange lines show approximately where the ice-shelf base is 50 and 100 m respectively above the seabed (Albert and Bentley, 1990). (b) Velocities measured in 2009 (Scheuchl and others, 2012) color-coded to show changes compared to those measured by RIGGS in 1975 (Thomas and others, 1984).

Velocities were also inferred from satellite SAR measurement in 1997 and 2009 with an accuracy of  $\sim\pm 6 \text{ m a}^{-1}$  (Scheuchl and others, 2012). Interferometric SAR (InSAR) data of the RIS were acquired during the 1997 RADARSAT-1 Antarctic Mapping Mission (RAMM) and the 2009 RADARSAT-2 mapping campaign. Imaging areas south of  $\sim 78^\circ \text{ S}$  requires left-looking capability. RADARSAT-1 acquisitions in 1997 were made in an experimental mode resulting in incomplete coverage of the area. The first, and so far only, complete coverage of central Antarctica with InSAR data was

achieved using RADARSAT-2 in left-looking mode in autumn 2009, with a limited gap-filler campaign to complete the mapping in 2011. This effort was part of an international Antarctic mapping campaign coordinated by the International Polar Year Space Task Group (Jezek and Drinkwater, 2008). The InSAR data were acquired with range and azimuth spacing of about 12 and 5 m, respectively. They were processed using a speckle-tracking technique (Michel and Rignot, 1999) to derive slant-range and azimuth displacements, which were subsequently converted to a



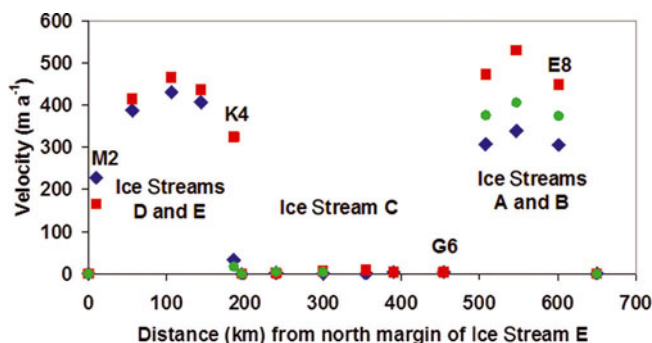


**Fig. 2.** Velocities measured across the section in Figure 1 near the grounding lines of ice streams flowing into the RIS from West Antarctica: in 1975 (red), 1997 (green) and 2009 (blue). At most stations, errors are estimated to be  $\sim 6 \text{ m a}^{-1}$  in 1997 and 2009, and  $\sim 30 \text{ m a}^{-1}$  in 1975.

two-dimensional velocity field (Scheuchl and others, 2012). The InSAR ice velocities were tide-corrected using the CATS2008a\_opt tide model (Padman and others, 2008) and the TPX06.2 load model (Egbert and Erofeeva, 2002).

We compared ICESat measurements from October/November 2003 with those from the same period in each year from 2004 to 2009, at orbit-crossing locations, and averaged resulting estimates of elevation-change rates ( $dS/dt$ ) over  $1^\circ$  latitude by  $10^\circ$  longitude 'grid squares'. Although these 'crossing-point' estimates are far more sparse than the commonly used 'repeat-track' comparisons (e.g. Pritchard and others, 2009, 2012), uncorrelated errors in area-averaged elevation change are smaller because ICESat orbit tracks do not exactly repeat, and repeat-track comparisons are 'blurred' by ice-surface slopes transverse to the orbit. However, far larger errors are introduced by a time-varying Geoscience Laser Altimeter System (GLAS) range error, probably resulting from variations among the different lasers aboard ICESat and progressive reduction in laser power. We corrected for these using ICESat measurements over the ocean, as described in Section 4. The ICESat measurements over the RIS were also corrected for tides from the TPX07.1 tide model (Egbert and Erofeeva, 2002).

A detailed analysis of the 1997 and 2009 InSAR-based velocity maps is provided by Scheuchl and others (2012). In addition to the reported deceleration of Ice Streams A (Mercer Ice Stream) and B (Whillans Ice Stream), the authors report a modest acceleration for Ice Stream D (Bindschadler Ice Stream) between 1997 and 2009 (up to 5% in speed over 12 years), as well as a modest deceleration for Ice Stream E (MacAyeal Ice Stream) of up to 7%. Velocity changes between 1997 and 2009 on the RIS are dominated by a slight acceleration seaward of Ice Stream D, and a larger deceleration of the western part of the ice shelf. Between 1975 and 2009, velocities decreased by almost  $200 \text{ m a}^{-1}$  close to the grounding lines of Ice Streams A and B in the southeast, continuing the trend observed between 1975 and 2004 (Joughin and others, 2002, 2005). But reductions were smaller further seaward, and little changed near the calving ice front. There was also a general clockwise shift of velocity direction, by several degrees in the southeast, and by  $2\text{--}4^\circ$  over most of the ice shelf.

Velocities close to the grounding lines of Ice Streams A and B decreased by  $143$  and  $191 \text{ m a}^{-1}$  respectively, with far smaller velocity decreases for Ice Streams D and E (Fig. 2), except at K4 and M2, where velocity changes suggest a

northward shift of both margins. For Ice Stream B, the deceleration rate was almost  $6 \text{ m a}^{-2}$  for 1975–97 and for 1997–2009. For Ice Stream A, however, deceleration increased from  $3.4 \text{ m a}^{-2}$  for 1975–97 to  $5.7 \text{ m a}^{-2}$  for 1997–2009. It appears that both ice streams are in transition from rapid motion to a state of near-stagnation similar to that of Ice Stream C (Kamb Ice Stream) further north, which ceased to be active  $\sim 160$  years ago (Retzlaff and Bentley, 1993). If they continue to slow down at these rates, both Ice Streams A and B will stagnate by 2060–70.

Ice-shelf thickness was also measured during RIGGS (Bentley and others, 1979), both at stations and along many flight lines, with errors estimated to be  $\pm 10 \text{ m}$ . We used these and the various velocity measurements to estimate the volume of ice discharged across sections near the ice-shelf grounding line, interpolating RIGGS velocity measurements linearly between stations. Velocity errors ranged from a few to  $\sim 30 \text{ m a}^{-1}$ , as discussed earlier, and we assumed these and thickness errors to be uncorrelated between stations. We used the RIGGS ice-thickness measurements for all time periods, assuming little change between the 1970s and 2009, to calculate volume discharge from the ice streams into the ice shelf, converting this to mass discharge assuming its density to be that of solid ice.

For Ice Streams A and B together, discharge decreased from  $46 \text{ Gt a}^{-1}$  to  $30 \text{ Gt a}^{-1}$  between 1975 and 2009. At all stations near the grounding line of Ice Stream C, velocities were very low (few  $\text{m a}^{-1}$ ), changing little throughout the observation period, and total discharge was  $< 1 \text{ Gt a}^{-1}$ . Ice Streams D and E flow into the ice shelf to the southeast of Roosevelt Island (Fig. 1), and here discharge decreased from  $45 \text{ Gt a}^{-1}$  to  $38 \text{ Gt a}^{-1}$  between 1975 and 1997, with little additional change between 1997 and 2009. The sharp velocity drop at the southern margin of Ice Streams D/E, and increase at the northern margin, suggest that the ice-stream margins are migrating northward, but the velocity estimates close to the southern margin have large errors. The RIGGS estimate, derived by using strain rates at K4 and nearby stations to interpolate between Geociever stations, had large errors because of high spatial variability in strain rates; the InSAR estimates for K4 could also have higher errors because of differing geocoding accuracy between RADAR-SAT-1 and -2.

Ice is also discharged into the RIS from the East Antarctic ice sheet (EAIS) via glaciers flowing through the Transantarctic Mountains. Our estimates of total discharge from the EAIS into the RIS decreased from  $\sim 56 \text{ Gt a}^{-1}$  in 1975 to  $\sim 52 \text{ Gt a}^{-1}$  in 2009, but the RIGGS velocity measurements were not well located for reliable interpolation, leading to errors that cannot be reliably assessed. Consequently, we cannot infer any significant change in ice discharge during the interim. However, InSAR measurements suggest a slight decrease in the velocity of Byrd Glacier and deceleration of the western part of the ice shelf between 1997 and 2009 (Scheuchl and others, 2012).

### 3. DECREASING ICE DISCHARGE INTO THE RIS FROM WEST ANTARCTICA

Based on the measurements shown in Figure 2 and RIGGS ice-thickness measurements, total discharge from Ice Streams A–C near their grounding lines was  $\sim 46 \text{ Gt a}^{-1}$  in 1975, falling to  $36 \text{ Gt a}^{-1}$  in 1997, and  $30 \text{ Gt a}^{-1}$  in 2009. For Ice Streams D and E (Fig. 3), velocity decrease implies that

ice discharge here dropped from  $\sim 45 \text{ Gt a}^{-1}$  to  $38 \text{ Gt a}^{-1}$  between 1975 and 2009. Total ice discharge into the RIS from Ice Streams A–E dropped from  $91 \text{ Gt a}^{-1}$  to  $68 \text{ Gt a}^{-1}$ . RIGGS measurements were too sparse to provide an accurate estimate of discharge from Ice Stream F (Echelmeyer Ice Stream) for 1975, but its discharge in 1997 and 2009 was only  $\sim 2 \text{ Gt a}^{-1}$  (Scheuchl and others, 2012).

Shabtaie and Bentley (1987, table 2c) estimated an overall mass balance of  $-17 \text{ Gt ice a}^{-1}$  in 1975 for the catchment basins of Ice Streams A–E, assuming total accumulation within catchment basins of  $76 \text{ Gt a}^{-1}$ , and discharge of  $93 \text{ Gt a}^{-1}$ . Using the Regional Atmospheric Climate Model (RACMO) accumulation rate for 1979–2010 (Lenaerts and others, 2012) of  $85 \text{ Gt a}^{-1}$ , and our estimated discharge for 1975 ( $91 \text{ Gt a}^{-1}$ ), we infer a mass balance of  $-6 \text{ Gt a}^{-1}$  (Table 1). The difference between the two estimates is almost totally caused by the big difference in the two estimates of snow accumulation in the A/B catchment basin.

The differences between total RACMO snow accumulation averaged over 1979–2010 and total ice discharge in 1975, 1997 and 2009 should give an indication of the long-term mass balance. Values in parentheses in Table 1 use RACMO estimates averaged over shorter periods close to the times of ice-discharge measurements, which we would expect to be more appropriate for comparison with mass balance inferred from ICESat measurements. However, the 2009 mass-budget estimates using 1979–2010 accumulation rates for Ice Streams C–E show better agreement with the ICESat estimates, casting doubt on the RACMO reduction in accumulation between 1979 and 2010. Moreover, the 2009 mass-budget estimates for A/B are substantially higher than the ICESat estimate, indicating that here the RACMO accumulation may be  $\sim 25\%$  too high. The ICESat measurements strongly suggest that this is the case, so our estimates for A/B and A–E mass balance should be decreased by  $8 \text{ Gt a}^{-1}$  to  $\sim -20 \text{ Gt a}^{-1}$  and  $\sim -14 \text{ Gt a}^{-1}$ , or approximately the same as the Shabtaie and Bentley (1987) estimates.

Table 1 shows a shift from strongly negative to near-balance for A/B with a similar trend for D/E, and a sustained

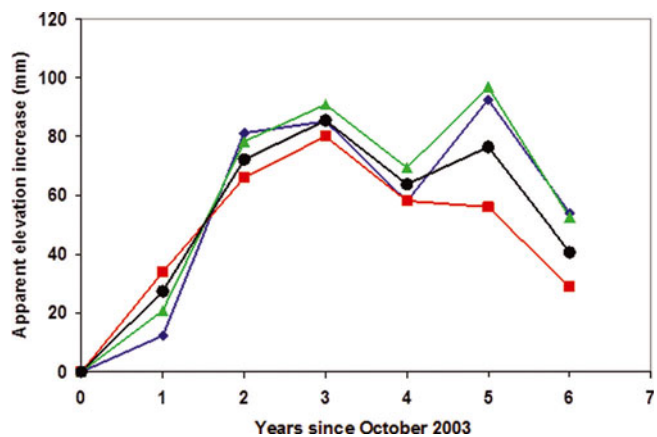


**Fig. 3.** Apparent increase in surface elevations of the ocean (red), corrected for a  $3 \text{ mm a}^{-1}$  rise in global sea level, and of high-altitude parts of the Antarctic ice sheet (blue, and green after correction for anomalous snowfall) inferred from ICESat surveys in October/November each year from 2003 to 2009. The black plot is the average of the red and green values, which we assumed to represent time-varying ICESat range bias.

positive balance for C. The mass balance of all ice streams, taken together, increased from strongly negative in 1975 to near-balance in 1997 to strongly positive in 2009, at a rate of  $\sim +0.7 \text{ Gt a}^{-2}$ , despite a substantial reduction in modeled snowfall after 1997. However, comparison of the mass-budget estimates with mass balance inferred from ICESat measurements stresses the need to check the RACMO accumulation estimates, particularly in the A/B catchment area and the rapidly decreasing snowfall modeled in all catchment basins after 1997.

#### 4. MASS BALANCE FROM ICESat MEASUREMENTS OF CHANGES IN SURFACE ELEVATION

Repeated ICESat surveys over the oceans reveal a time-variable range bias (Gunter and others, 2008; Urban, 2010), which is broadly consistent with our observations over

**Table 1.** Ice discharge into the RIS from Ice Streams A–E, for 1975, 1997 and 2009, with associated input from snow accumulation. Mass-budget estimates are differences between 1979–2010 RACMO accumulation rates (Lenaerts and others, 2012) and ice discharge, with values in parentheses using accumulation rates most appropriate to the velocity measurement periods (e.g. value for 1997 uses 9210: the average for 1992–2010). Also shown are mass-balance estimates derived from repeated ICESat measurements at orbit crossovers. All units are  $\text{Gt a}^{-1}$ . The mass-budget estimates in italics were calculated assuming snow accumulation in the A/B catchment basin is  $8 \text{ Gt a}^{-1}$  lower than the RACMO 7910 value, resulting in a 2009 mass-budget estimate in agreement with that inferred from ICESat measurements. Uncertainty for 2009 mass-budget values assumes velocity errors of  $6 \text{ m a}^{-1}$  on InSAR estimates and  $30 \text{ m a}^{-1}$  on RIGGS estimates, ice thickness errors of 20 m and accumulation rate errors of 7%, but clearly the latter appear to be grossly underestimated for the A/B catchment. For ICESat estimates, errors are based only on the goodness of fit of straight-line fits, and do not include uncertainty in assumed density

Ice stream	Ice discharge				Snow accumulation				Mass balance ( $dM/dt$ )				ICESat	
	1975	S&B*	1997	2009	7910	9210	0510	S&B*	1975	S&B*	1997	2009	$\pm$	2003–09 $\pm$
A–B	45.9	46.3	36.3	30.0	34.0 26.0	34.3	32.3	23.2	-11.9 -19.9	-23.1	-2.3 (-2.0) -10.3	4.0 (2.3) -4.0	3	-4 1
C	0.3	2.1	0.3	0.3	17.3	16.8	15.0	+18.7	+17.0	16.6	17.0 (16.5)	17.0 (14.7)	2	19 3
D–E	44.8	44.7	38.2	37.8	34	34.4	30.6	34.5	-10.8	-10.2	-4.2 (-3.8)	-3.8 (-7.2)	3	0 1
A–E	91.0	93.1	74.8	68.1	85.3 77.3	85.5	77.9	76.4	-5.7 -13.7	-16.7	10.5 (10.7) 2.5	17.2 (9.8) 9.2	5	15 4

\*From Shabtaie and Bentley (1987).

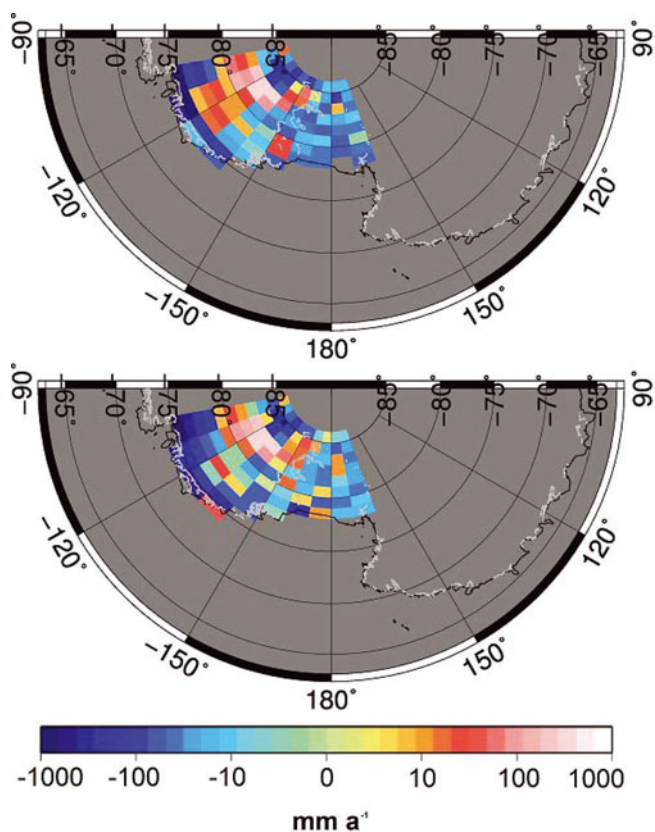


**Fig. 4.** Rates of surface-elevation change ( $dS/dt$ ) inferred from ICESat data for 2003–07 (top), and 2003–09 (bottom). Ice-shelf grounding lines are shown in pale gray.

high-elevation parts of the ice sheet where accumulation rates and interannual variability are extremely small (Fig. 3).

Comparison of the range bias for each observation period with that for the earliest survey in 2003 gave the rate of change in range bias (the 'range-bias drift') which we used to correct our  $dS/dt$  estimates to the grid-square averages shown in Figure 4, with standard errors of a few  $\text{mm a}^{-1}$ , except in generally near-coastal regions with high spatial variability of  $dS/dt$ . Our estimates of range-bias drift decrease from  $\sim 3 \text{ cm a}^{-1}$  over the first 3 years of the ICESat mission to  $< 1 \text{ cm a}^{-1}$  between 2003 and late 2009, in contrast to the constant value of  $2 \text{ cm a}^{-1}$  adopted by Gunter and others (2009) and Riva and others (2009). The importance of this correction is highlighted by the fact that 1 cm elevation change over the  $650\,000 \text{ km}^2$  area of the A–E catchment basins represents a volume change of  $6.5 \text{ km}^3$ .

We converted the rates of surface-elevation change shown in Figure 4 to estimates of volume-change rate on the WAIS by multiplying by the grid-square area, and we summed these over each of the catchment basins listed in Table 1. In order to convert these to estimates of mass balance (Fig. 5), we used the density of solid ice, assuming observed changes to be caused by long-term changes to the ice sheet, and yielding upper limits to resulting mass changes. If, however, the changes were caused by short-term snowfall variability, the density could be far lower, reducing mass changes by as much as 50%, which could partially explain differences between our estimates in Table 1 of mass budget in 2009 and those for 2003–09 from ICESat.

The mass-budget estimates using the RACMO accumulation estimates for 1979–2010 in Table 1 for 2009 show agreement, within estimated errors, with mass-balance estimates for 2003–09 inferred from the ICESat measurements except for Ice Streams A/B, where the ICESat estimate is  $8 \text{ Gt a}^{-1}$  lower than the comparison of input with 2009 outflow. RACMO estimates, showing snowfall over the A/B catchment basin decreasing with time (Table 1), cannot explain the  $8 \text{ Gt a}^{-1}$  difference. Although the A/B catchment basin includes  $\sim 30\,000 \text{ km}^2$  that is south of the  $86^\circ \text{ S}$  limit of ICESat coverage, ice within the A/B basin between  $84^\circ$  and  $86^\circ \text{ S}$  thinned by  $> 10 \text{ cm a}^{-1}$ , suggesting that nearly all the basin is thinning. Consequently, we conclude that actual accumulation rates in the A/B catchment area may be considerably lower than the RACMO estimates, as suggested in Section 3.

Our ICESat estimate of  $dM/dt$  for Ice Streams D–E in Table 1 is based on the straight-line fit in Figure 5, but the data show positive  $dM/dt$  between 2003.8 and 2005.8, followed by  $dM/dt \sim -3 \text{ Gt a}^{-1}$  thereafter, in closer agreement with the mass-budget estimate for 1997 and 2009 of  $\sim -4 \text{ Gt a}^{-1}$ .

Pritchard and others (2009) estimated  $dM/dt \sim +36 \text{ Gt a}^{-1}$  from ICESat repeat-track measurements for 2003–07 over the entire catchment basin of Ice Streams A–F for 2003–07, which is considerably higher than our estimate of  $\sim +21 \text{ Gt a}^{-1}$  for the same period. But this is largely because Pritchard and others (2009) did not apply corrections for ICESat range drift of  $\sim 16 \text{ mm a}^{-1}$  between 2003 and 2007, leading to overestimation by  $\sim 10 \text{ Gt a}^{-1}$  of the mass balance within the A–E catchment basins.

Over the RIS, we find broadly the same pattern of thickening and thinning as range-drift corrected ICESat results shown by Pritchard and others (2012). Thinning predominates over most of the freely floating ice shelf, with quite rapid thickening on the 'ice plain' where Ice Streams A and B enter the ice shelf. This thickening is consistent with the continued slowdown of these ice streams. However, our observations (Fig. 6) suggest that thickening rates may be decreasing. Average  $dS/dt \sim -2.5 \text{ cm a}^{-1}$  over most of the ice shelf implies thinning by  $\sim 20 \text{ cm a}^{-1}$ , consistent with increasing longitudinal strain rates and creep thinning. Figure 1 shows 2009 velocities near the RIS seaward ice front to be almost the same as in 1975, whereas those 500 km inland decreased by  $\sim 100 \text{ m a}^{-1}$ , implying an increase in longitudinal strain rates by  $\sim 0.0002 \text{ a}^{-1}$ , and in creep thinning of 400 m thick ice shelf by  $\sim 8 \text{ cm a}^{-1}$ . This suggests that either creep thinning was already  $\sim 12 \text{ cm a}^{-1}$  in 1975, or that basal melting was  $\sim 12 \text{ cm a}^{-1}$ .

## 5. THE FUTURE

Our results show substantial thickening of the southeast corner of the RIS, which must increase resistance to ice-stream flow, because of increased basal drag as more of the ice-shelf weight is supported by the locally grounded regions, and as these regions grow in size over near-horizontal seabed that is probably undergoing isostatic uplift following comparatively recent WIS retreat. With an area of several thousand  $\text{km}^2$ , the ice plain increases resistance to the flow of both Ice Streams A and B, and lower reaches of the slowing ice streams thicken, which increases friction between the ice plain and its bed, further slowing the ice streams (Thomas and others, 1988). Although other processes, such as changes in basal melting and freezing (Hulbe and Fahnestock, 2004;



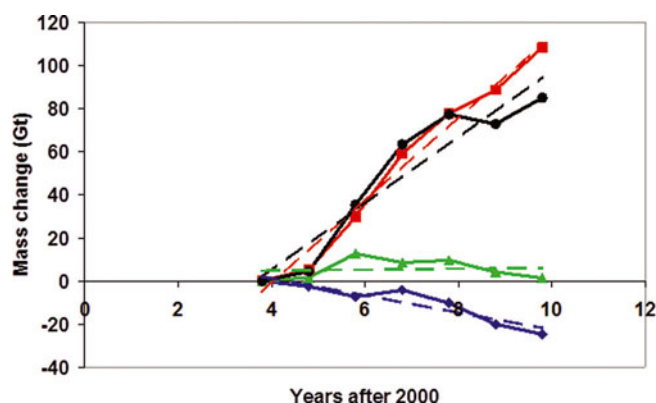


**Fig. 5.** Mass balance for the catchment basins of Ice Streams A–E, inferred from ICESat surveys in October/November 2003–09, corrected for a time-variable laser range bias. Ice Streams A/B: blue; C: red; D–E: green; A–E: black. Straight-line fits imply  $dM/dt \sim -4 \text{ Gt a}^{-1}$  for A/B;  $+19 \text{ Gt a}^{-1}$  for C; 0 for D–E; and  $+15 \text{ Gt a}^{-1}$  for A–E.

Catania and others, 2006, 2012; Beem and others, 2010), probably contribute to the velocity decrease, the ice plain is undoubtedly thickening, which must increase basal drag over grounded parts of the ice plain.

The rapid slowdown of Ice Streams A and B should favour ice-shelf thinning by the combined effects of reduced advection of thicker ice from the slowing ice streams, ice-shelf basal melting and an increase in longitudinal creep rates as buttressing from the slowing ice shelf decreases. Indeed, despite the rapid slowdown of the RIS in the southeast, ice velocities near the ice front were almost the same in 2009 as in 1975 (Fig. 1), implying an increase in creep-thinning rates by almost  $10 \text{ cm a}^{-1}$ , which would at least partially explain the ice-shelf thinning inferred from ICESat surveys (Pritchard and others, 2012), and shown here in Figure 6.

If Ice Streams A and B continue to slow at recent rates, it is quite likely that, as the ice shelf thins, its calving front will retreat, further reducing its buttressing, which would favour increased creep thinning of the ice shelf and possible flotation of the ice plains. This, in turn, would reduce buttressing forces on the ice streams, leading to an increase in ice-stream discharge. Indeed, a cycle of ice-stream deceleration followed by acceleration may be an inevitable consequence of shoaling seabed near the grounding lines of Ice Streams A–C, with each cycle modulated by the effects of sea-level rise, isostatic uplift of the seabed, and deposition of sediment from the ice streams as they become afloat (Thomas and others, 1988). Moreover, this cycle may not be in phase for each ice stream. Ice Stream C ceased to be active in the mid-1800s, whereas slowdown of A and B is quite recent.

## 6. CONCLUSIONS

Our analysis of RIGGS and InSAR measurements shows continued slowing of Ice Streams A and B flowing into the southeast part of the Ross Ice Shelf, sufficient to shift the balance of the western part of the WAIS from  $-14 \text{ Gt a}^{-1}$  in 1975 to growth by  $9 \text{ Gt a}^{-1}$  in 2009. Ice discharge into the RIS from East Antarctica totals  $\sim 50 \text{ Gt a}^{-1}$ , and showed no significant change between 1975 and 2009. We also find little change in ice velocities near the seaward ice front of the RIS, implying an increase in longitudinal strain rates over

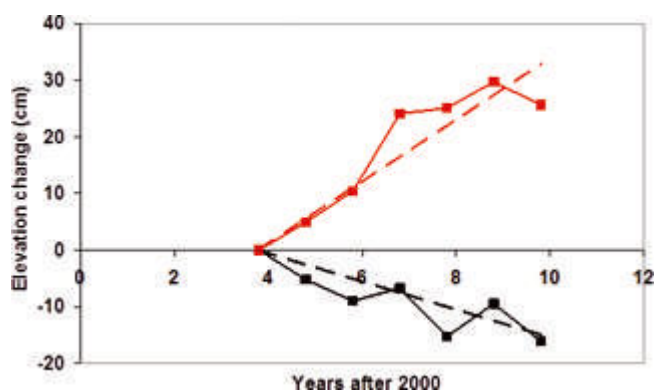


**Fig. 6.** Changes in surface elevation averaged over freely floating parts of the RIS (black) and over the partially grounded 'ice plain' (red), where Ice Streams A and B enter the ice shelf. The straight lines correspond to  $dS/dt \sim -2.5 \text{ cm a}^{-1}$  for floating ice shelf and  $\sim +5.5 \text{ cm a}^{-1}$  on the ice plain, with uncertainty of  $\sim \pm 0.5 \text{ cm a}^{-1}$ .

much of the ice shelf. Comparison of ICESat measurements between 2003 and 2009, corrected for a drift in measured laser ranges during the mission, confirms overall thickening of the western part of the WAIS except in the catchment basin of Ice Stream A, which is thinning quite rapidly. The ICESat measurements also show substantial thickening of the partially grounded southeastern part of the RIS, and slow thinning of much of the rest of the ice shelf, consistent with an increase in longitudinal strain rates on the freely floating ice shelf.

## ACKNOWLEDGEMENTS

We thank C. Bentley for helping us to track down some of the RIGGS results, two reviewers and particularly the Scientific Editor, Ted Scambos, for suggesting improvements to the paper, and NASA's Cryospheric Research Program for funding support. The generation of InSAR-based ice velocity and grounding line was supported by NASA's MEASUREs (Making Earth Science Data Records for Use in Research Environments) program.

## REFERENCES

- Albert DG and Bentley CR (1990) Seismic studies on the grid-eastern half of the Ross Ice Shelf: RIGGS III and RIGGS IV. In Hayes D and Bentley CR eds. *The Ross Ice Shelf: glaciology and geophysics*. (Antarctic Research Series 42) American Geophysical Union, Washington, DC, 87–108
- Beem LH, Jezek KC and Van der Veen CJ (2010) Basal melt rates beneath Whillans Ice Stream, West Antarctica. *J. Glaciol.*, **56**(198), 647–654 (doi: 10.3189/002214310793146241)
- Bentley CR (1984) The Ross Ice Shelf Geophysical and Glaciological Survey (RIGGS): introduction and summary of measurements performed. In Hayes D and Bentley CR eds. *The Ross Ice Shelf: glaciology and geophysics*. (Antarctic Research Series 42) American Geophysical Union, Washington, DC, 1–20
- Bentley CR, Clough JW, Jezek KC and Shabtaie S (1979) Ice-thickness patterns and the dynamics of the Ross Ice Shelf, Antarctica. *J. Glaciol.*, **24**(90), 287–294
- Catania GA, Scambos TA, Conway H and Raymond CF (2006) Sequential stagnation of Kamb Ice Stream, West Antarctica. *Geophys. Res. Lett.*, **33**(14), L14502 (doi: 10.1029/2006GL026430)

- Catania G, Hulbe C, Conway H, Scambos TA and Raymond CF (2012) Variability in the mass flux of the Ross ice streams, West Antarctica, over the last millennium. *J. Glaciol.*, **58**(210), 741–752 (doi: 10.3189/2012JoG11J219)
- Egbert GD and Erofeeva SY (2002) Efficient inverse modeling of barotropic ocean tides. *J. Atmos. Ocean. Technol.*, **19**(2), 183–204 (doi: 10.1175/1520-0426(2002)019<0183:EIMOBO>2.0.CO;2)
- Fahnestock MA, Scambos TA, Bindschadler RA and Kvaran G (2000) A millennium of variable ice flow recorded by the Ross Ice Shelf, Antarctica. *J. Glaciol.*, **46**(155), 652–664 (doi: 10.3189/172756500781832693)
- Gunter B and 6 others (2008) Evaluation of GRACE and ICESat mass change estimates over Antarctica. In Merkitas SP ed. *Proceedings of the IAG International Symposium on Gravity, Geoid and Earth Observation (GGEO), 23–27 June 2008, Chania, Greece*. (International Association of Geodesy Commission 2) Springer, Berlin
- Gunter B and 9 others (2009) A comparison of coincident GRACE and ICESat data over Antarctica. *J. Geod.*, **83**(11), 1051–1060 (doi: 10.1007/s00190-009-0323-4)
- Hulbe CL and Fahnestock MA (2004) West Antarctic ice-stream discharge variability: mechanism, controls and pattern of grounding-line retreat. *J. Glaciol.*, **50**(171), 471–484 (doi: 10.3189/172756504781829738)
- Jezek K and Drinkwater MR (2008) International viewpoint and news – global interagency IPY polar snapshot year: an update. *Environ. Geol.*, **55**(6), 1379–1380 (doi: 10.1007/s00254-008-1393-y)
- Joughin I, Tulaczyk S, Bindschadler RA and Price S (2002) Changes in West Antarctic ice stream velocities: observation and analysis. *J. Geophys. Res.*, **107**(B11), 2289 (doi: 10.1029/2001JB001029)
- Joughin I and 10 others (2005) Continued deceleration of Whillans Ice Stream, West Antarctica. *Geophys. Res. Lett.*, **32**(22), L22501 (doi: 10.1029/2005GL024319)
- Lenaerts JTM, Van den Broeke MR, Van de Berg WJ, Van Meijgaard E and Kuipers Munneke P (2012) A new, high-resolution surface mass balance map of Antarctica (1979–2010) based on regional atmospheric climate modeling. *Geophys. Res. Lett.*, **39**(4), L04501 (doi: 10.1029/2011GL050713)
- Michel R and Rignot E (1999) Flow of Glaciar Moreno, Argentina, from repeat-pass Shuttle Imaging Radar images: comparison of the phase correlation method with radar interferometry. *J. Glaciol.*, **45**(149), 93–100
- Padman L, Erofeeva SY and Fricker HA (2008) Improving Antarctic tide models by assimilation of ICESat laser altimetry over ice shelves. *Geophys. Res. Lett.*, **35**(22), L22504 (doi: 10.1029/2008GL035592)
- Pritchard HD, Arthern RJ, Vaughan DG and Edwards LA (2009) Extensive dynamic thinning on the margins of the Greenland and Antarctic ice sheets. *Nature*, **461**(7266), 971–975 (doi: 10.1038/nature08471)
- Pritchard HD, Ligtenberg SRM, Fricker HA, Vaughan DG, Van den Broeke MR and Padman L (2012) Antarctic ice-sheet loss driven by basal melting of ice shelves. *Nature*, **484**(7395), 502–505 (doi: 10.1038/nature10968)
- Retzlaff R and Bentley CR (1993) Timing of stagnation of Ice Stream C, West Antarctica, from short-pulse radar studies of buried surface crevasses. *J. Glaciol.*, **39**(133), 553–561
- Rignot E, Mouginot J and Scheuchl B (2011) Antarctic grounding line mapping from differential satellite radar interferometry. *Geophys. Res. Lett.*, **38**(10), L10504 (doi: 10.1029/2011GL047109)
- Riva R and 9 others (2009) Glacial isostatic adjustment over Antarctica from combined ICESat and GRACE satellite data. *Earth Planet Sci. Lett.*, **288**(3–4), 516–523 (doi: 10.1016/j.epsl.2009.10.013)
- Scheuchl B, Mouginot J and Rignot E (2012) Ice velocity changes in the Ross and Ronne sectors observed using satellite radar data from 1997 and 2009. *Cryosphere*, **6**(5), 1019–1030 (doi: 10.5194/tc-6-1019-2012)
- Shabtaie S and Bentley CR (1987) West Antarctic ice streams draining into the Ross Ice Shelf: configuration and mass balance. *J. Geophys. Res.*, **92**(B2), 1311–1336 (doi: 10.1029/JB092iB02p01311)
- Stephenson SN and Bindschadler RA (1988) Observed velocity fluctuations on a major Antarctic ice stream. *Nature*, **334**(6184), 695–697 (doi: 10.1038/334695a0)
- Thomas RH (1976) Thickening of the Ross Ice Shelf and equilibrium state of the West Antarctic ice sheet. *Nature*, **259**(5540), 180–183 (doi: 10.1038/259180a0)
- Thomas RH, MacAyeal DR, Eilers DH and Gaylor DR (1984) Glaciological studies on the Ross Ice Shelf, Antarctica, 1973–1978. In Hayes D and Bentley CR eds. *The Ross Ice Shelf: glaciology and geophysics*. (Antarctic Research Series 42) American Geophysical Union, Washington, DC, 21–53
- Thomas RH, Stephenson SN, Bindschadler RA, Shabtaie S and Bentley CR (1988) Thinning and grounding-line retreat on Ross Ice Shelf, Antarctica. *Ann. Glaciol.*, **11**, 165–172
- Urban T (2010) Estimation and implication of ICESat inter-campaign elevation biases derived over the global oceans. [Abstr. C41A-0488] Am. Geophys. Union, Fall Meeting <http://adsabs.harvard.edu/abs/2010AGUFM.C41A0488U>

MS received 8 August 2012 and accepted in revised form 6 May 2013.